31st Congress of the International Council of the Aeronautical Sciences

Belo Horizonte, Brazil; September 09-14, 2018

ADAPTIVE OUTPUT-FEEDBACK GAIN SCHEDULING APPLIED TO FLEXIBLE AIRCRAFT

Rafael M. Bertolin* , **Antônio B. Guimarães Neto*** , **Guilherme C. Barbosa*** , **Flávio J. Silvestre***

***Instituto Tecnológico de Aeronáutica, São José dos Campos, SP, 12228-900, Brazil**

Keywords: *Adaptive control, flexible aircraft, MRAC, X-HALE*

Abstract

The advantages of full-state feedback adaptive control in dealing with uncertainties of a flexible aircraft model are demonstrated with the use of model reference adaptive control. Design of an output-feedback system with an observer, based on the separation principle, is attempted. Differences in both stability and performance characteristics of the full-state feedback and the output-feedback closed-loop systems demonstrate that further investigation is needed to design adaptive output-feedback controllers.

1 Introduction

Flexible aircraft (FA) are caracterized by low or very low frequencies of their aeroelastic modes and, as a consequence, strong, dangerous and undesirable coupling between the structural dynamics and the rigid-body flight dynamics may occur. For example, the short-period mode of a very FA can become unstable as the dihedral angle increases [1].

A special class of FA that has motivated the scientific community in recent decades is known as High-Altitude Long-Endurance (HALE) aircraft. The mission profile of a HALE aircraft involves cruising at very high altitudes (above 20 km) and flying for weeks, months and even years [2]. It turns out that, due to the mission requirements, these aircraft may undergo actuator anomalies such as power surge in motors or structural damage in control surfaces.

The described adversities give rise to a series of challenges in the flight control law design process [3] and may sometimes exceed the stability margins of the system. In such cases, traditional linear control techniques are no longer adequate. On the other hand, adaptive control is an appropriate solution because it should be able to overcome all these adversities [4].

In this paper, the advantages of adaptive control in dealing with uncertainties of a control system applied to flexible aircraft will be demonstrated for an experimental HALE aircraft, the X-HALE [5].

At first and assuming that all the system states are measurable, a linear baseline control system for velocity, altitude, sideslip and roll angle tracking will be designed and afterwards augmented by a model reference adaptive control (MRAC) law [6]. A comparison between the two systems (with and without the MRAC augmentation) will be made by which the usefulness of the adaptive controller will become apparent.

At a second moment and to address the state feedback problem, an attempt to design an observer based on the separation principle will be performed.

2 Problem Statement

The FA flight dynamics under small disturbances around an equilibrium flight condition can be represented by a class of multi-input multi-output (MIMO) linear time-invariant (LTI) uncertain

systems in the following form:

$$\dot{\mathbf{x}}_\mathbf{p} = \mathbf{A_p}\mathbf{x_p} + \mathbf{B_p}\Lambda\left[\mathbf{u} + \Theta^T\Phi(\mathbf{x_p})\right] \quad (1)$$

$$\mathbf{y_p} = \mathbf{C_p}\mathbf{x_p} + \mathbf{D_p}\Lambda\left[\mathbf{u} + \Theta^T\Phi(\mathbf{x_p})\right] \quad (2)$$

where $\mathbf{x_p} \in \mathbb{R}^{n_x}$ corresponds to the state vector, $\mathbf{u} \in \mathbb{R}^{n_u}$ are the control inputs, $\mathbf{y_p} \in \mathbb{R}^{n_y}$ is the system output vector, composed of measurement outputs ($\mathbf{y_m} \in \mathbb{R}^{n_m}$) and tracking outputs ($\mathbf{y_t} \in \mathbb{R}^{n_t}$) that are also measured, according to:

$$\underbrace{\begin{bmatrix}\mathbf{y_m}\\ \mathbf{y_t}\end{bmatrix}}_{\mathbf{y_p}} = \underbrace{\begin{bmatrix}\mathbf{C_m}\\ \mathbf{C_t}\end{bmatrix}}_{\mathbf{C_p}}\mathbf{x_p} + \underbrace{\begin{bmatrix}\mathbf{D_m}\\ \mathbf{D_t}\end{bmatrix}}_{\mathbf{D_p}}\Lambda\left[\mathbf{u} + \Theta^T\Phi(\mathbf{x_p})\right] \quad (3)$$

The matrices $\mathbf{A_p} \in \mathbb{R}^{n_x \times n_x}$, $\mathbf{B_p} \in \mathbb{R}^{n_x \times n_u}$, $\mathbf{C_m} \in \mathbb{R}^{n_m \times n_x}$, $\mathbf{C_t} \in \mathbb{R}^{n_t \times n_x}$, $\mathbf{D_m} \in \mathbb{R}^{n_m \times n_u}$ and $\mathbf{D_t} \in \mathbb{R}^{n_t \times n_u}$ are assumed to be constant and known. This assumption corresponds to an ideal case. In reality, several types of uncertainties exist in the dynamic model and such matrices are unknown and even time-variant.

Aiming at inserting more realism into the ideal system, two kinds of parametric uncertainties are considered in Eqs. (1) and (2): an unknown constant multiplicative diagonal matrix $\Lambda \in \mathbb{R}^{n_u \times n_u}$ with strictly positive diagonal elements, to represent control actuator uncertainties, control effectiveness reduction and other control failures, damage or anomalies; and an additive term $\mathbf{f}(\mathbf{x_p}) = \Theta^T\Phi(\mathbf{x_p})$ that represents uncertainties present in $\mathbf{A_p}$ through the input channels, where $\mathbf{f}(\cdot) : \mathbb{R}^{n_x} \to \mathbb{R}^{n_u}$, $\Theta \in \mathbb{R}^{n_x \times n_u}$ is a matrix of unknown constant parameters and $\Phi(\mathbf{x_p}) \in \mathbb{R}^{n_x}$ is a known regressor vector.

The control problem is to design $\mathbf{u}$ such that $\mathbf{y_t}$ tracks a bounded time-variant reference signal $\mathbf{y_{cmd}}$ in the presence of the aforementioned constant parametric uncertainties, whereas the rest of the signals in the closed-loop system as well as tracking errors remain bounded.

3 Control Design

In face of the problem described in section 2, the control signal $\mathbf{u}$ is selected as:

$$\mathbf{u} = \mathbf{u_{bl}} + \mathbf{u_{ad}} \quad (4)$$

where $\mathbf{u_{bl}}$ corresponds to a baseline linear controller and $\mathbf{u_{ad}}$ is an MRAC.

The reason for using this augmentation approach (baseline + adaptive) stems from the fact that in most realistic applications a system already has a baseline controller designed to operate under (or very close to) nominal conditions. When subjected to excessive disturbances this controller has its performance degraded. In such situations, the adaptive term acts to recover the desired performance (and ensure stability) by means of an online adjustment and in a real-time fashion [6].

This section presents the methodologies used to design $\mathbf{u_{bl}}$ and $\mathbf{u_{ad}}$: section 3.1 shows the architecture and the design procedure of the baseline linear control system, which will also serve as reference model in the design of the adaptive control law described in section 3.2.

In the following section $\mathbf{u_{bl}}$ will be designed in the form of a full state feedback. This corresponds to assume that all states are available for feedback. Evidently, this assumption constitutes a practical limitation of the designed control law because the states of a system usually cannot be completely measured. However, the design of output-feedback based controllers for nonlinear uncertain MIMO systems represents a challenging problem [6]. Regarding adaptive controllers, these challenges represent several restrictive assumptions that the plant has to fulfill. Recent research [7, 8] relaxed these assumptions, but the complexity of the problem remains. To address this issue, an attempt to apply the separation principle [9] will be investigated in more detail in section 5.

Moreover, the pair $(\mathbf{A_p}, \mathbf{B_p})$ is assumed controllable and $(\mathbf{A_p}, \mathbf{C_m})$ observable. Controllability is necessary to ensure model matching conditions of the adaptive law, which will be explained in section 3.2. Observality is necessary for the analysis of section 5.

3.1 Baseline Control Design

For the purpose of tracking with null steady state error, the baseline control system corresponds to

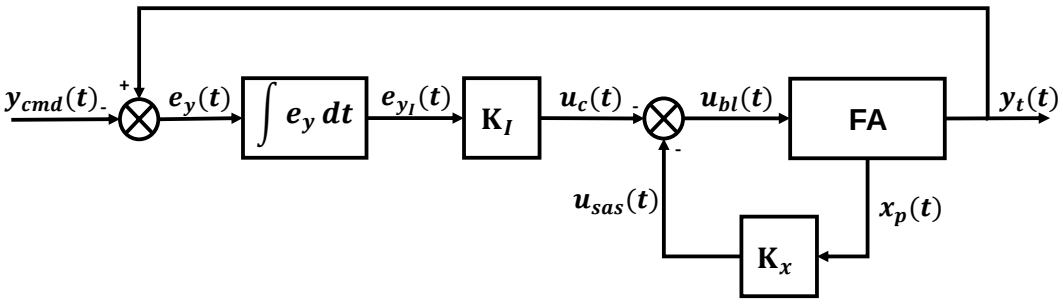

Fig. 1 Baseline linear control system block diagram.

a linear quadratic regulator (LQR) with proportional and integral feedback connections (Figure 1) [10].

Let $\mathbf{y_{cmd}} \in \mathbb{R}^{n_t}$ be a bounded command that $\mathbf{y_t}$ must track and $\mathbf{e_y} = \mathbf{y_t} - \mathbf{y_{cmd}}$ be the output tracking error whose integral is denoted by $\mathbf{e_{y_I}}$:

$$\dot{\mathbf{e}}_{\mathbf{y_I}} = \mathbf{e_y} = \mathbf{y_t} - \mathbf{y_{cmd}} \tag{5}$$

From Eqs. (1), (3) and (5), the extended open-loop dynamics can be written as:

$$\underbrace{\begin{bmatrix} \dot{\mathbf{e}}_{\mathbf{y_I}} \\ \dot{\mathbf{x}}_\mathbf{p} \end{bmatrix}}_{\dot{\mathbf{x}}} = \underbrace{\begin{bmatrix} \mathbf{0} & \mathbf{C_t} \\ \mathbf{0} & \mathbf{A_p} \end{bmatrix}}_{\mathbf{A}} \underbrace{\begin{bmatrix} \mathbf{e}_{\mathbf{y_I}} \\ \mathbf{x_p} \end{bmatrix}}_{\mathbf{x}} + \underbrace{\begin{bmatrix} -\mathbf{I} \\ \mathbf{0} \end{bmatrix}}_{\mathbf{B_{ref}}} \mathbf{y_{cmd}} + \underbrace{\begin{bmatrix} \mathbf{D_t} \\ \mathbf{B_p} \end{bmatrix}}_{\mathbf{B}} \Lambda[\mathbf{u} + \mathbf{f}(\mathbf{x_p})] \tag{6}$$

In terms of the tracking outputs:

$$\underbrace{\mathbf{y_t}}_{\mathbf{y}} = \underbrace{\begin{bmatrix} \mathbf{0} & \mathbf{C_t} \end{bmatrix}}_{\mathbf{C}} \begin{bmatrix} \mathbf{e}_{\mathbf{y_I}} \\ \mathbf{x_p} \end{bmatrix} + \underbrace{\mathbf{D_t}}_{\mathbf{D}} \Lambda[\mathbf{u} + \mathbf{f}(\mathbf{x_p})] \tag{7}$$

Equations (6) and (7) can be written compactly as:

$$\dot{\mathbf{x}} = \mathbf{A}\mathbf{x} + \mathbf{B}\Lambda[\mathbf{u} + \mathbf{f}(\mathbf{x_p})] + \mathbf{B_{ref}}\mathbf{y_{cmd}} \tag{8}$$

$$\mathbf{y} = \mathbf{C}\mathbf{x} + \mathbf{D}\Lambda[\mathbf{u} + \mathbf{f}(\mathbf{x_p})] \tag{9}$$

The baseline control law is designed assuming that the system operates in the nominal conditions. It corresponds to set $\Lambda = \mathbf{I}$ and $\Theta = \mathbf{0}$ in the previous equations, resulting in the linear baseline open-loop system:

$$\dot{\mathbf{x}} = \mathbf{A}\mathbf{x} + \mathbf{B}\mathbf{u_{bl}} + \mathbf{B_{ref}}\mathbf{y_{cmd}} \tag{10}$$

$$\mathbf{y} = \mathbf{C}\mathbf{x} + \mathbf{D}\mathbf{u_{bl}} \tag{11}$$

where:

$$\mathbf{u_{bl}} = -\underbrace{\begin{bmatrix} \mathbf{K_I} & \mathbf{K_x} \end{bmatrix}}_{\mathbf{K^T}} \mathbf{x} = -\mathbf{K^T}\mathbf{x} \tag{12}$$

It is well-known [11] that the optimal LQR solution is given by:

$$\mathbf{K^T} = \mathbf{R^{-1}}\mathbf{B^T}\mathbf{P} \tag{13}$$

with $\mathbf{P}$ being the unique symmetric positive-definite solution of the algebraic Riccati equation (ARE):

$$\mathbf{A^T}\mathbf{P} + \mathbf{P}\mathbf{A} + \mathbf{Q} - \mathbf{P}\mathbf{B}\mathbf{R^{-1}}\mathbf{B^T}\mathbf{P} = \mathbf{0} \tag{14}$$

which is solved using the symmetric positive-denite design parameters $\mathbf{Q}$ and $\mathbf{R}$.

Therefore, the baseline closed-loop system is given by:

$$\dot{\mathbf{x}} = \left(\mathbf{A} - \mathbf{B}\mathbf{K^T}\right)\mathbf{x} + \mathbf{B_{ref}}\mathbf{y_{cmd}} \tag{15}$$

$$\mathbf{y} = \left(\mathbf{C} - \mathbf{D}\mathbf{K^T}\right)\mathbf{x} \tag{16}$$

3.2 MRAC Design

The adaptive control law that composes the total control input (Eq. 4) is based on the MRAC approach [6, 12].

The baseline closed-loop dynamic given by Eq. (15) corresponds to the desired behavior for the actual closed-loop system. Therefore, the reference model is assumed to be:

$$\dot{\mathbf{x}}_{\mathbf{ref}} = \mathbf{A_{ref}}\mathbf{x_{ref}} + \mathbf{B_{ref}}\mathbf{y_{cmd}} \tag{17}$$

$$\mathbf{y_{ref}} = \mathbf{C_{ref}}\mathbf{x_{ref}} \tag{18}$$

where:

$$\mathbf{A_{ref}} = \mathbf{A} - \mathbf{BK^T} \tag{19}$$

$$\mathbf{C_{ref}} = \mathbf{C} - \mathbf{DK^T} \tag{20}$$

correspond to the model matching conditions and must be ensured.

As previously stated, the adaptive term in Eq. (4) acts to recover the desired behavior for the actual closed-loop system when operating in the presence of uncertainties or disturbances, and must be designed in such a way that the dynamics in Eq. (8) when under the effect of the input given in Eq. (4) matches Eq. (17). So, substituting Eq. (4) into (8):

$$\dot{\mathbf{x}} = \mathbf{Ax} + \mathbf{B}\Lambda\left[\mathbf{u_{bl}} + \mathbf{u_{ad}} + \Theta^T\Phi(\mathbf{x_p})\right] + \mathbf{B_{ref}y_{cmd}} \tag{21}$$

From Eqs. (12), (19) and (21):

$$\dot{\mathbf{x}} = \mathbf{A_{ref}x} + \mathbf{B}\Lambda\left[\mathbf{u_{ad}} + \overbrace{\left(\mathbf{I} - \Lambda^{-1}\right)}^{\mathbf{K_u^T}}\mathbf{u_{bl}} + \Theta^T\Phi(\mathbf{x_p})\right] + \mathbf{B_{ref}y_{cmd}} \tag{22}$$

which can be rewritten as:

$$\dot{\mathbf{x}} = \mathbf{A_{ref}x} + \mathbf{B}\Lambda\left[\mathbf{u_{ad}} + \bar{\Theta}^T\bar{\Phi}(\mathbf{u_{bl}}, \mathbf{x_p})\right] + \mathbf{B_{ref}y_{cmd}} \tag{23}$$

with:

$$\bar{\Theta}^T = \begin{bmatrix} \mathbf{K_u^T} & \Theta^T \end{bmatrix} \tag{24}$$

$$\bar{\Phi}(\mathbf{u_{bl}}, \mathbf{x_p}) = \begin{bmatrix} \mathbf{u_{bl}} \\ \Phi(\mathbf{x_p}) \end{bmatrix} \tag{25}$$

Equivalently:

$$\mathbf{y} = \mathbf{C_{ref}x} + \mathbf{D}\Lambda\left[\mathbf{u_{ad}} + \bar{\Theta}^T\bar{\Phi}(\mathbf{u_{bl}}, \mathbf{x_p})\right] \tag{26}$$

Comparing Eqs. (23) and (26) with (17) and (18), respectively, it is evident that if the adaptive law $\mathbf{u_{ad}}$ is chosen to dominate the system uncertainties $\bar{\Theta}^T\bar{\Phi}(\mathbf{u_{bl}}, \mathbf{x_p})$, $\mathbf{x} \to \mathbf{x_{ref}}$ and consequently $\mathbf{y} \to \mathbf{y_{ref}}$. Therefore, proposing:

$$\mathbf{u_{ad}} = -\hat{\bar{\Theta}}^T\bar{\Phi}(\mathbf{u_{bl}}, \mathbf{x_p}) \tag{27}$$

where $\hat{\bar{\Theta}} \in \mathbb{R}^{(n_u+n_x)\times n_u}$ corresponds to the matrix of adaptive parameters, defining the matrix of parameter estimation error as:

$$\Delta\bar{\Theta} = \hat{\bar{\Theta}} - \bar{\Theta} \tag{28}$$

and substituting Eq. (27) into Eqs. (23) and (26) results in:

$$\dot{\mathbf{x}} = \mathbf{A_{ref}x} - \mathbf{B}\Lambda\Delta\bar{\Theta}^T\bar{\Phi}(\mathbf{u_{bl}}, \mathbf{x_p}) + \mathbf{B_{ref}y_{cmd}} \tag{29}$$

$$\mathbf{y} = \mathbf{C_{ref}x} - \mathbf{D}\Lambda\Delta\bar{\Theta}^T\bar{\Phi}(\mathbf{u_{bl}}, \mathbf{x_p}) \tag{30}$$

Introducing the state tracking error as:

$$\mathbf{e} = \mathbf{x} - \mathbf{x_{ref}} \tag{31}$$

the state tracking error dynamics can now be calculated by subtracting the reference model dynamics in Eq. (17) from the actual closed-loop extended system in Eq. (29):

$$\dot{\mathbf{e}} = \mathbf{A_{ref}e} - \mathbf{B}\Lambda\Delta\bar{\Theta}^T\bar{\Phi}(\mathbf{u_{bl}}, \mathbf{x_p}) \tag{32}$$

It is possible to demonstrate using Lyapunov's direct method (Ref. [6], chapter 10) that, if the adaptive law is chosen in the form:

$$\dot{\hat{\bar{\Theta}}} = \Gamma_{\bar{\Theta}}\bar{\Phi}(\mathbf{u_{bl}}, \mathbf{x_p})\mathbf{e}^T\mathbf{P_{ref}B} \tag{33}$$

then the closed-loop state tracking error dynamics in Eq. (32) is globally asymptotically stable. In other words, the closed-loop system from Eq. (29) globally asymptotically tracks the reference model from Eq. (17), as $t \to \infty$ and for any bounded command $\mathbf{y_{cmd}}$. At the same time, $\mathbf{y}$ (Eq. (30)) also track $\mathbf{y_{cmd}}$ with bounded errors.

In Eq. (33), $\Gamma_{\bar{\Theta}} = \Gamma_{\bar{\Theta}}^T > 0$ represents rates of adaptation and $\mathbf{P_{ref}} = \mathbf{P_{ref}}^T > 0$ is the unique symmetric positive-definite solution of the algebraic Lyapunov equation:

$$\mathbf{A_{ref}}^T\mathbf{P_{ref}} + \mathbf{P_{ref}A_{ref}} = -\mathbf{Q_{ref}} \tag{34}$$

where $\mathbf{Q_{ref}} = \mathbf{Q_{ref}}^T > 0$ is a matrix of design parameters.

4 Numerical Application

This section presents a numerical application of the formulation developed in the previous section. Section 4.1 introduces the flexible aircraft considered here, the X-HALE. Section 4.2 addresses the model order reduction for control purpose. Lastly, section 4.3 describes the design procedure and the simulation cases analyzed.

4.1 The X-HALE Aircraft

The X-HALE is a radio-controlled unmanned experimental airplane developed to be a test platform to collect aeroelastic data coupled with the aircraft rigid-body motion, in order to validate mathematical formulations of flexible-aircraft flight dynamics as well as control system design techniques [5].

It can be configured to fly as a four-, six- or eight-meter-span configuration. In all of them, the outer panels of the wing have 10 degree dihedral angle. A central stabilizer is used with a flipping mode (horizontal or vertical position) to increase or decrease lateral-directional stability of the aircraft. In this work, the four-meter-span configuration is considered, only. Figure 2 illustrates the aircraft.

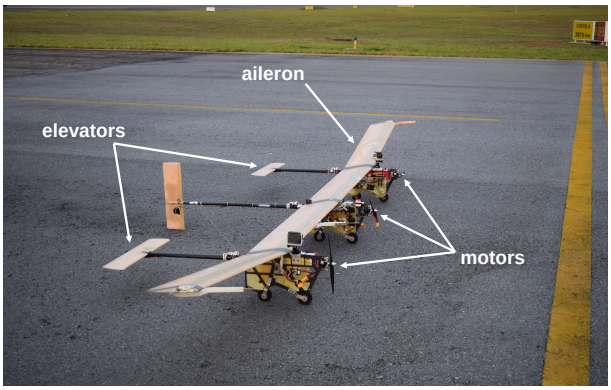

Fig. 2 Four-meter-span, vertical-central-tail X-HALE configuration.

The mathematical formulation employed to model the X-HALE flight dynamics was developed by Guimarães Neto [13].

The state variables of the full nonlinear model are given by:

$$\mathbf{x_{full}} = \begin{bmatrix} V & \alpha & q & \theta & H & x & \beta & \phi & p & r & \psi & y & \cdots \\ & & & & & & & & & & & & \\ & & & & & & & & & & & & \lambda_{rb}{}^T \ \eta^T \ \dot{\eta}^T \ \lambda_\eta{}^T \end{bmatrix}^T \quad (35)$$

The model includes the kinematic equations in the inertial reference frame, for all six degrees of freedom: displacements in the x and y directions, altitude H and roll, pitch and yaw angles (ϕ, θ and ψ, respectively). Furthermore, the velocity V, the angle of attack α, the sideslip angle β, as well as the angular rates p, q and r also have their corresponding equations of motion. A particular feature of the model is the modeling of the structural dynamics using modal amplitudes and their time-derivatives (η and $\dot{\eta}$). Modes of vibration with frequencies up to 25 Hz are retained in the model. Aerodynamic lag states arise due to rigid-body and control-surface dynamics ($\lambda_{\mathbf{rb}}$) and due to the aeroelastic dynamics (λ_η). Therefore, the full model is composed of 210 states: 12 from rigid body motion plus 63 from rigid-body and control-surface aerodynamic lag states plus 30 from aeroelastic states plus 105 from aeroelastic aerodynamic lag states.

The four-meter-span aircraft is composed of two boom-mounted elevators, two ailerons and three motors. All these actuators can be independently controlled. However, to accomplish aircraft control in a more conventional way, the longitudinal attitude is controlled by the elevators (δ_e), the rolling motion is controlled by the ailerons (δ_a), whereas the yawing motion is controlled using differential thrust of the external motors (δ_r). The global thrust level of the three motors responds to the throttle command (δ_t). Then, the input vector can be rewritten as:

$$\mathbf{u} = \begin{bmatrix} \delta_t & \delta_e & \delta_a & \delta_r \end{bmatrix}^T \quad (36)$$

The output vector $\mathbf{y_p} \in \mathbb{R}^{90\times 1}$ comprises model outputs such as displacements and attitudes, linear and angular velocities, load factors, at different points of the wing and close to the center of gravity (CG) of the aircraft. The measurements made possible by the aircraft sensors are a subset of the model outputs.

The full nonlinear model may be linearized around different equilibrium conditions. In this paper, all subsequent development is performed considering linearized models around the straight and level flight condition with velocity of 14 m/s and altitude of 650 meters, ISA+10. Moreover, the full linear model (around such flight condition) of the vertical-central-tail configuration aircraft is assumed as the nominal open-loop model.

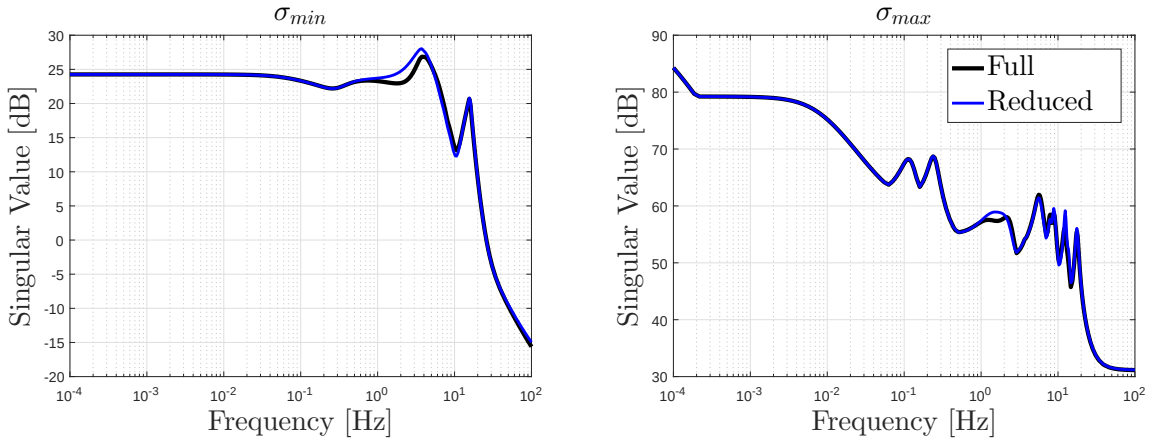

Fig. 3 Comparison between the maximum and minimum singular values of the transfer function matrices for both full and reduced models.

4.2 Model Reduction

The high order of the X-HALE model is a challenge to most of the control techniques and therefore a state-space reduced-order model is appropriate. For this purpose, a residualization technique is applied to all the aerodynamic lag states of the nominal model [13]. The resulting reduced linear model ($\mathbf{A_p}$, $\mathbf{B_p}$, $\mathbf{C_p}$, $\mathbf{D_p}$) comprises nine rigid-body states of the full model (discarding ignorable variables x, y and ψ) as well as the aeroelastic ones:

$$\mathbf{x_p} = \left[V \;\; \alpha \;\; q \;\; \theta \;\; H \;\; \beta \;\; \phi \;\; p \;\; r \;\; \eta^T \;\; \dot{\eta}^T \right]^T \quad (37)$$

totalizing thirty-nine states. Fig. 3 examines the maximum and minimum singular values of the MIMO transfer function matrix for both full and reduced models. It is notorious that the reduced model preserves sufficient characteristics of the full one. This makes sense, since the aerodynamic lag states have a greater impact on the phase of the system.

4.3 Simulation Results

In order to illustrate the advantages of the MRAC augmentation of a baseline linear controller, a control system for velocity, altitude, sideslip and roll angle tracking is considered.

From the reduced linear model, the first step is to obtain the augmented open-loop dynamics, according to Eq. (10), including the integral of the following output tracking error:

$$\mathbf{e_y} = \mathbf{y_t} - \mathbf{y_{cmd}} = \begin{bmatrix} V \\ H \\ \phi \\ \beta \end{bmatrix} - \begin{bmatrix} V_{cmd} \\ H_{cmd} \\ \phi_{cmd} \\ \beta_{cmd} \end{bmatrix} \quad (38)$$

The baseline linear controller is then designed from Eqs. (12), (13) and (14), with the appropriate choices for the ARE parameters:

$$\mathbf{Q} = \begin{bmatrix} \mathbf{I}_{4\times4} & \mathbf{0}_{4\times39} \\ \mathbf{0}_{39\times4} & 10^{-3}\mathbf{I}_{39\times39} \end{bmatrix} \quad (39)$$

$$\mathbf{R} = diag\,(25,\ 0.1,\ 0.1,\ 25) \quad (40)$$

where $diag\,(\bullet)$ is a diagonal matrix for which the main diagonal elements are given by $\bullet$.

The next step is to design the MRAC system (from Eqs. (34) and (33)) in order to recover the desired closed-loop performance given by Eqs. (17) and (18). After some iterations focusing on a fast tracking with reduced transient oscillations, the following parameters were selected:

$$\mathbf{Q_{ref}} = 10^{-3} \begin{bmatrix} \mathbf{I}_{4\times4} & \mathbf{0}_{4\times9} & \mathbf{0}_{4\times30} \\ \mathbf{0}_{9\times4} & 10^{-2}\mathbf{I}_{9\times9} & \mathbf{0}_{9\times30} \\ \mathbf{0}_{30\times4} & \mathbf{0}_{30\times9} & 10^{-1}\mathbf{I}_{30\times30} \end{bmatrix} \quad (41)$$

$$\Gamma_{\bar{\Theta}} = 5 * 10^{-3} \begin{bmatrix} \mathbf{I}_{4\times4} & \mathbf{0}_{4\times39} \\ \mathbf{0}_{39\times4} & \mathbf{I}_{39\times39} \end{bmatrix} \quad (42)$$

with $\Phi(\mathbf{x_p}) = \mathbf{x_p}$ being the choice for the regression vector of Eq. (25) [6].

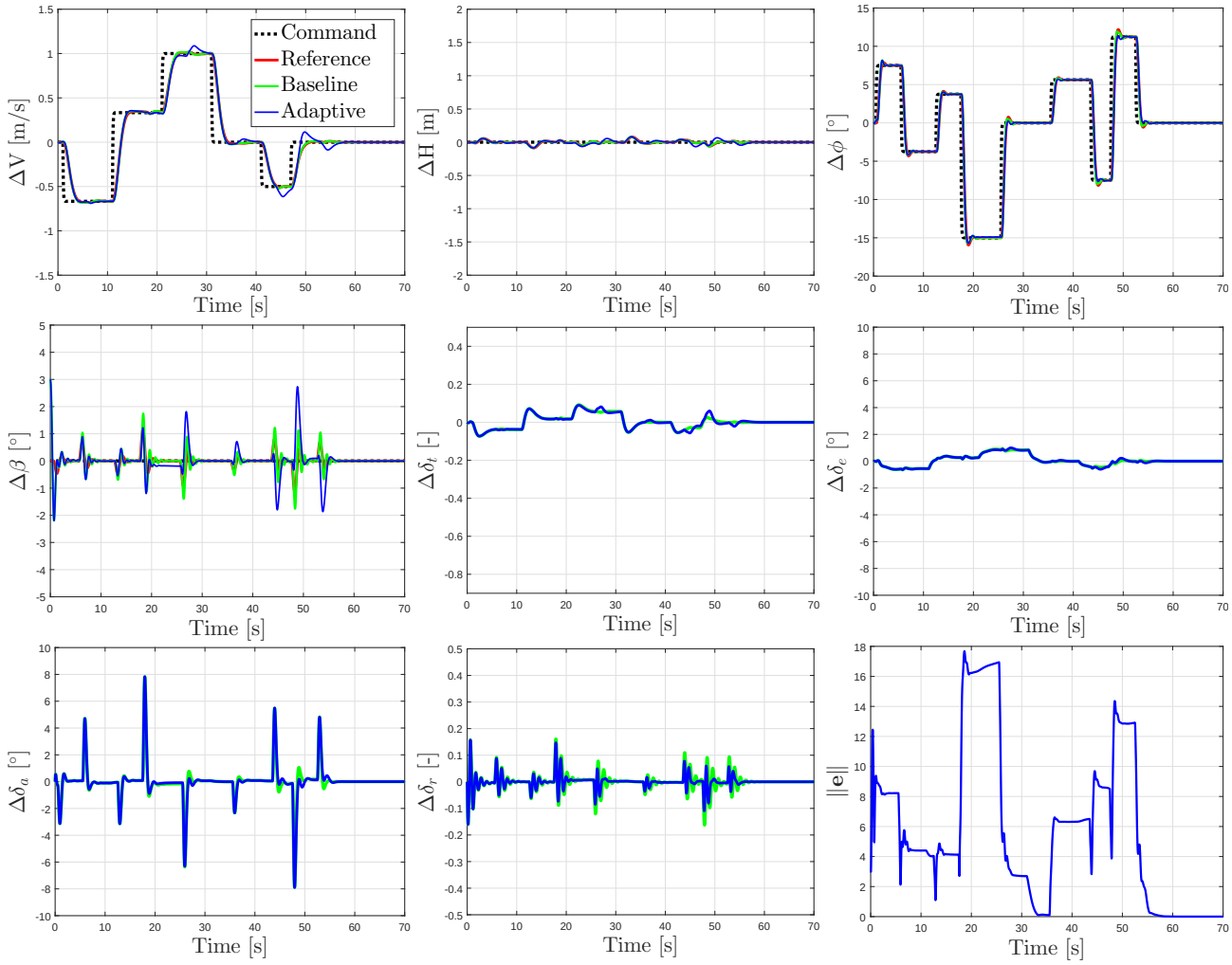

Fig. 4 Simulation results of the case **(i)** (vertical-central-tail aircraft in nominal condition).

To validate the designed controller as well as to demonstrate the potentiality of the adaptive control, three cases are analyzed: **(i)** considering the vertical-central-tail aircraft operating in the nominal condition, that is, straight and level flight at 14 m/s and 650 meters; **(ii)** considering the horizontal-central-tail aircraft also flying at 14 m/s and 650 meters, however after a damage of the right motor; **(iii)** the same flight condition as in (ii) but with the residual effectiveness of the right motor degraded.

Some aspects of the previous cases deserve attention: **(1)** in all of them the simulations are performed using the respective full linear model. As a consequence, the effects of the aerodynamic lag states are treated as model parametric uncertainties; **(2)** the simulations consider the dynamics as well as the saturation of the actuators, whereas the design was carried out without both. All actuator dynamics are first-order functions, with time constant of 75 ms for the control surfaces and 150 ms for the motors. For the control surfaces, the saturation magnitude is ± 8 deg, for the rudder $\pm 30\%$ of the throttle command and for the throtlle $[30\%, -70\%]$. These limits correspond to the maximum possible perturbations around the equilibrium condition; **(3)** about the fault tolerance test of cases (ii) and (iii), it was assumed that, to represent some sort of damage to the right motor, its maximum throttle command was limited to 50%, and therefore the aircraft assumed a new equilibrium condition. This represents a new set of matrices $\mathbf{A_p}$, $\mathbf{B_p}$, $\mathbf{C_p}$ and $\mathbf{D_p}$; **(4)** another uncertainty present in this new set of matrices corresponds to the horizontal-central-tail configuration of the aircraft; **(5)** lastly, in (iii),

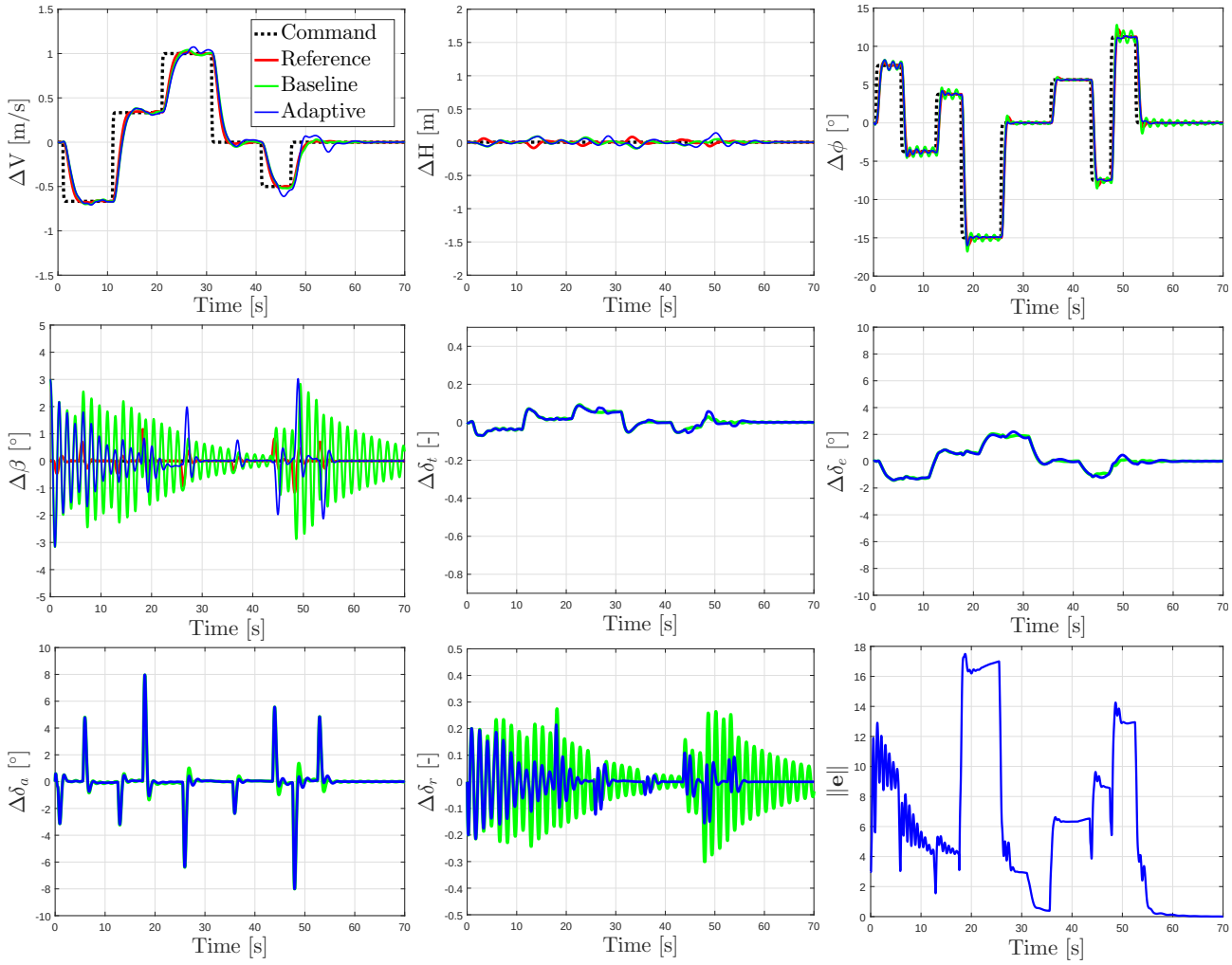

Fig. 5 Simulation results of the case **(ii)** (horizontal-central-tail aircraft after a right motor damage).

the residual effectiveness of the right motor is degraded by a factor $\Lambda = 0.85$.

The simulation results are presented in Figures 4 to 7, where the curves called *Reference* correspond to the reference model response, the *Baseline* curves are the response of the closed-loop system considering $\mathbf{u} = \mathbf{u_{bl}}$ (just the baseline control law) and the curves called *Adaptive* are the response of the closed-loop system considering $\mathbf{u} = \mathbf{u_{bl}} + \mathbf{u_{ad}}$ (baseline + adaptive control laws).

It is desired to track velocity (V_{cmd}) and roll angle (ϕ_{cmd}) commands, while the commanded altitude (H_{cmd}) and sideslip (β_{cmd}) are kept constant and equal to zero. An initial condition of $\beta(0) = 3°$ is considered.

Figure 4 shows the simulation results of case (i). In an ideal case, the reference, baseline and adaptive curves must be identical, once without uncertainties the reference model is exactly the baseline linear control system, and therefore the term $\mathbf{u_{ad}}$ must remain null. It turns out that the simulation model for this case contains some parametric uncertainties, and this is probably the reason for the mismatch between the curves. Even so, both (baseline and adaptive) perform very similarly to the reference model. Regarding the control signals, it is observed that all of them are feasible, that is, they operate with magnitudes smaller than the stipulated limits and presenting feasible rates. Lastly, is is possible to see that the 2-norm of the state tracking error tends asymptotically to zero, as expected.

Figure 5 shows the simulation results of case (ii). For this case, it is observed that the uncertainties of the model have a significant influence.

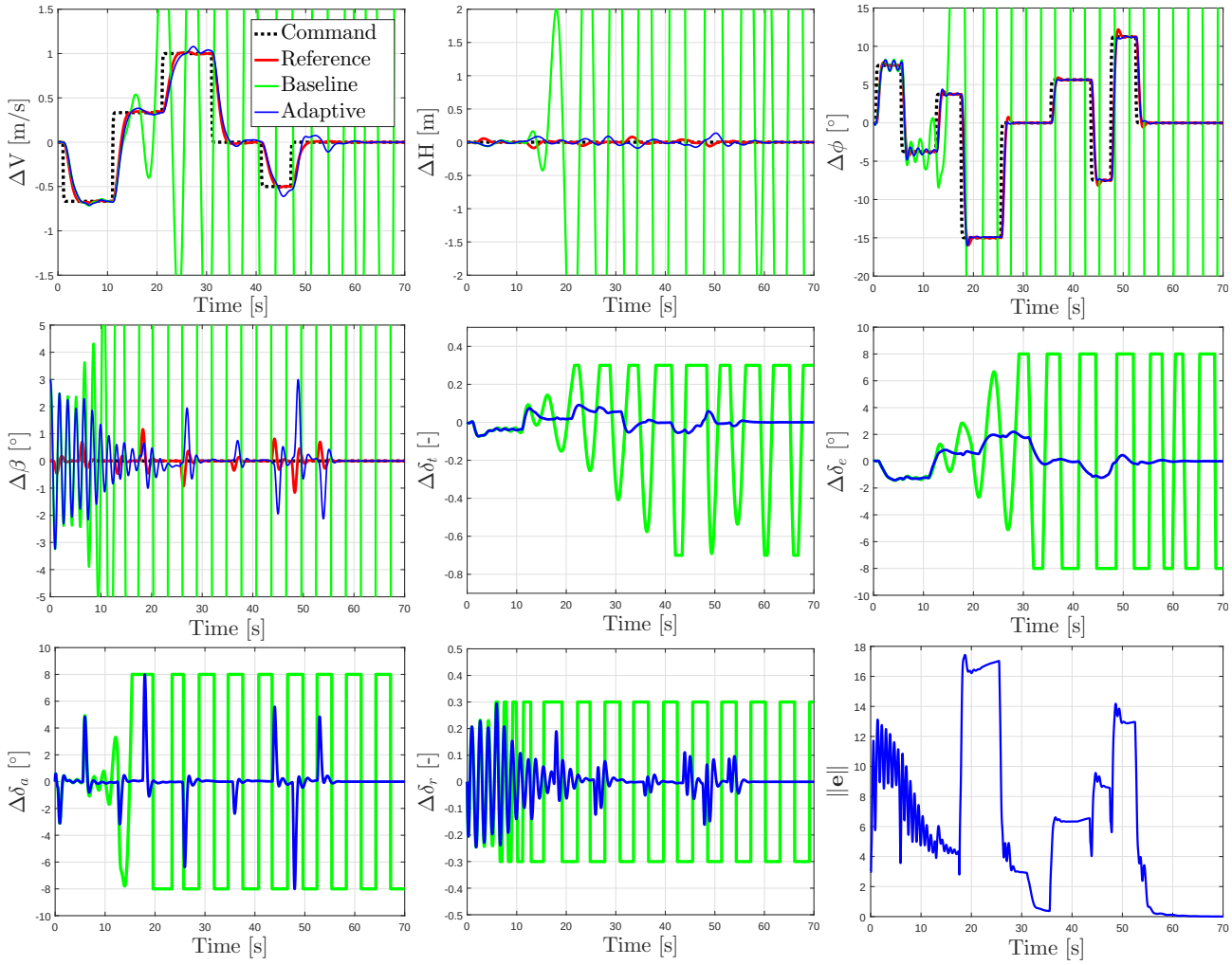

Fig. 6 Simulation results of the case **(iii)** (horizontal-central-tail aircraft after a right motor damage and residual effectiveness degradation).

Although the baseline system still performs satisfactorily, its response is clearly compromised. Among all the uncertainties considered, the failure of the right motor is the most critical, and its impacts are evident, as clearly seen in the evolution of β and δ_r. More differential thrust is needed to compensate the asymmetric failure. A direct consequence of the right motor damage is the worsening of the β regulation. On the other hand, the adaptive controller performs much better and indicates its usefulness in dealing with problems of this nature. Once more the 2-norm of the state tracking error tends asymptotically to zero.

Case (iii) is certainly the most interesting of all, and the simulation results are presented in Figure 6. In addition to preserving all the parametric uncertainties of case (ii), the right motor has its residual effectiveness degraded by a multiplicative factor of 0.85. In this case the baseline control system diverges. However, the MRAC not only ensures stability of the closed-loop system, but also very good performance, with feasible control signals. Only β presents some oscillations in the initial instants. The 2-norm of the state tracking error remains converging to zero. Figure 7 presents the temporal evolution of the 2-norm of the adaptive gain vectors with respect to each one of the control inputs. Note that with the asymptotic convergence to zero of the state tracking error 2-norm, the 2-norm of the adaptive gain vectors tends to a steady state value.

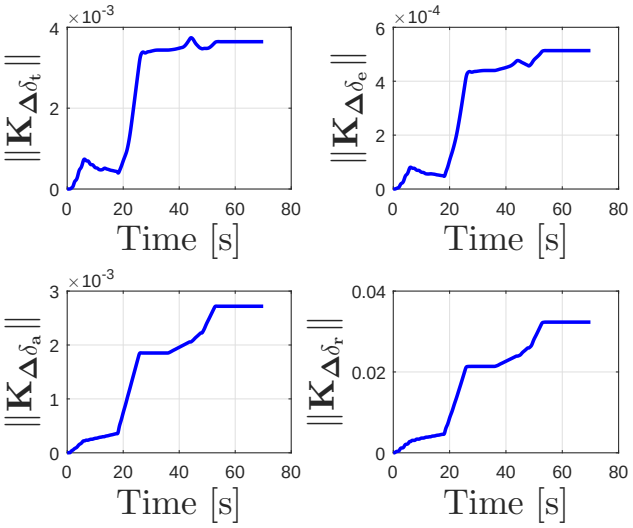

Fig. 7 Temporal evolution of the 2-norm of the adaptive gain vectors with respect to each of the control channels. Results of case (iii).

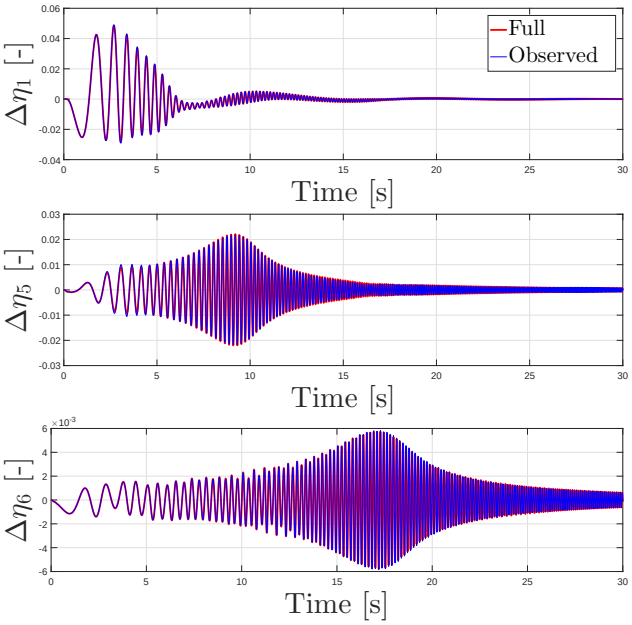

Fig. 8 Observer response versus full-order model for coupled sinusoidal elevator (0.1 to 15 Hz) and aileron (0.1 to 10 Hz) commands.

5 Observer-Based Adaptive Controllers

In linear control theory, a very well-established approach to deal with the practical problem of designing an output-feedback controller is the separation principle, according to which a full-state-variable feedback can be coupled to an observer that provides state estimates based on a reduced number of measurements [9]. There are even works where such an approach was applied to the control of flexible aircraft [14].

The question that arises is whether the application of such principle together with adaptive control technique remains valid. In general, the separation principle does not exist for nonlinear control systems [15]. Some works on the separation principle in adaptive control can be cited [16, 17]. However no global stability results are reported. In Ref. [15] an alternative and much more promising approach is proposed in which the author makes use of a closed-loop reference model as an observer and ensures global stability under certain assumptions.

In this section, an attempt is made to employ the separation principle together with the MRAC. The observer here proposed is designed according to Ref. [14] and the detailed theory about this approach can be found in Ref. [9].

To observe the states of the reduced model (section 4.2), acceleration measurements in the three axes as well as angular rates (p, q and r) are taken from three different points of the aircraft: left and right wing tips and close to CG. In addition, strain gauges located in both the right and left wing are also considered. Observability of the system considering such measurements was checked. Choosing weighting matrices $10^{-3}\mathbf{I}_{39\times 39}$ for the observer states and $10^{2}\mathbf{I}_{27\times 27}$ for the measurements, the observer gain matrix $\mathbf{L}$ is calculated.

Figure 8 shows the comparison between the observer response and the full-order linear model, for coupled sinusoidal elevator (0.1 to 15 Hz) and aileron (0.1 to 10 Hz) commands. The first, fifth and sixth aeroelastic states are presented. They correspond to the first torsion and bending modes. It is noticed that the observer generates good estimates of the states. The case (ii) simulation results considering now the observer in the loop are presented in Figure 9.

Regarding the MRAC law, the closed-loop system remains stable but has its performance much degraded. On the other hand, the baseline controller that, in case (ii), assuming full

state feedback, is stable and presents good performance, is unstable for the case in which the observer is considered.

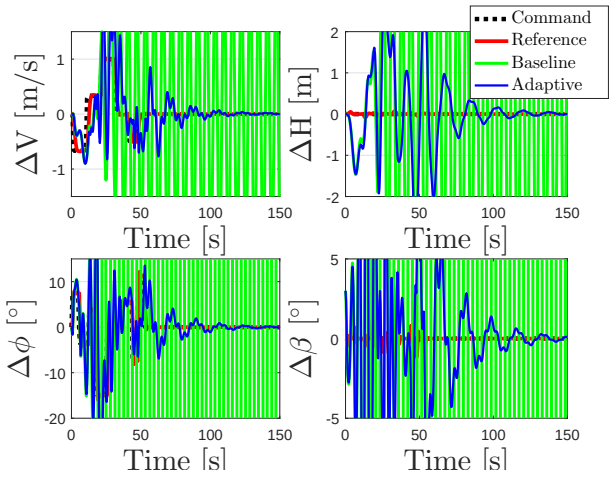

Fig. 9 Simulation results of the case **(ii)**, but considering the observer in the loop.

6 Conclusions

This paper aimed at demonstrating the advantages of the MRAC in dealing with uncertainties of a control system applied to the X-HALE aircraft. A comparison between the linear baseline control system and the MRAC augmentation was performed in which the usefulness of the adaptive controller is evident.

A discussion on the use of the separation principle with the MRAC was presented. It has been verified that the observer inclusion is able to destabilize the baseline control system subject to uncertainties, whereas the adaptive one ensures stability but with degraded performance.

It is clear that further investigation is necessary to develop an adaptive output-feedback control system that is both stable and of performance comparable to that of full-state feedback.

Contact Author Email Address

rafaelmbufsj@gmail.com

Acknowledgement

This work has been funded by FINEP and EMBRAER under the research project Advanced Studies in Flight Physics, contract number 01.14.0185.00.

Copyright Statement

The authors confirm that they, and/or their company or organization, hold copyright on all of the original material included in this paper. The authors also confirm that they have obtained permission, from the copyright holder of any third party material included in this paper, to publish it as part of their paper. The authors confirm that they give permission, or have obtained permission from the copyright holder of this paper, for the publication and distribution of this paper as part of the ICAS proceedings or as individual off-prints from the proceedings.

References

[1] Gibson, T., Annaswamy, A. M. and Lavretsky, E. Modeling for control of very flexible aircraft. *In: AIAA Guidance, Navigation, and Control Conference*, p. 6202, 2011.

[2] D' Oliveira, F. A., Melo, F. C. L. and Devezas, T. C. High-altitude platforms-present situation and technology trends. *Journal of Aerospace Technology and Management*, v. 8, n. 3, pp. 249-262, 2016.

[3] Gadient, R., Lavretsky, E. and Wise, K. A. Very flexible aircraft control challenge problem. *In: AIAA Guidance, Navigation, and Control Conference*, p. 4973, 2012.

[4] Zheng, Q. and Annaswamy, A. M. Adaptive output-feedback control with closed-loop reference models for very flexible aircraft. *Journal of Guidance, Control, and Dynamics*, v. 39, n. 4, pp. 873-888, 2015

[5] Cesnik, C. E. S., Senatore, P. J., Su, W., Atkins, E. M. and Shearer, C. M. X-HALE: a very flexible unmanned aerial vehicle for nonlinear aeroelastic tests. *AIAA Journal*, v. 50, n. 12, 2012.

[6] Lavretsky, E. and Wise, K. A. *Robust and Adaptive Control*. Advanced Textbooks in Control

and Signal Processing, DOI: 10.1007/978-1-4471-4396-3_1, Springer, 2013.

[7] Zheng, Q., Annaswamy, A. M. and Lavretsky, E. Adaptive output-feedback control for relative degree two systems based on closed-loop reference models. *In: IEEE Annual Conference on Decision and Control*, pp. 7598-7603, 2015.

[8] Zheng, Q., Annaswamy, A. M. and Lavretsky, E. Adaptive output-feedback control for a class of multi-input-multi-output plants with applications to very flexible aircraft. *In: IEEE American Control Conference*, 2016.

[9] Stevens, B. L. and Lewis, F. L. *Aircraft Control and Simulation*. 2nd edition, Wiley-India, 2010.

[10] Franklin, G. F., Powell, J. D. and Emami-Naeini, A. *Feedback Control of Dynamic Systems*. 6th edition, Prentice Hall, 2009.

[11] Anderson, B. D. O. and Moore, J. B. *Optimal Control, Linear Quadratic Methods*. Mineola, 2007.

[12] Narendra, K. S. and Annaswamy, A. M. *Stable Adaptive Systems*. Courier Corporation, 2012.

[13] Guimarães Neto, A. B. *Flight dynamics of flexible aircraft using general body axes: a theoretical and computational study*. Instituto Tecnológico de Aeronáutica. São José dos Campos: ITA, 2014.

[14] Silvestre, F. J., Guimarães Neto, A. B., Bertolin, R. M., Silva, R. G. and Paglione, P. Aircraft control based on flexible aircraft dynamics. *Journal of Aircraft*, v. 54, n. 1, pp. 262-271, 2017.

[15] Gibson, T., Zheng, Q., Annaswamy, A. M. and Lavretsky, E. Adaptive Output feedback based on closed-loop reference model. *IEEE Transactions on Automatic Control*, v. 60, n. 10, pp. 2728-2733, 2015.

[16] Khalil, H. K. Adaptive Output feedback control of nonlinear systems represented by input-output models. *IEEE Transactions on Automatic Control*, v. 41, n. 2, pp. 177-188, 1996.

[17] Atassi, A. N. and Khalil, H. K. A separation principle for the control of a class of nonlinear systems. *IEEE Transactions on Automatic Control*, v. 46, n. 5, pp. 742-746, 2001.